

Bradykinin antagonist dimer, CU201, inhibits the growth of human lung cancer cell lines by a “biased agonist” mechanism

Daniel Chan^{*††}, Lajos Gera^{*§}, John Stewart^{*§}, Barbara Helfrich^{*†}, Marileila Verella-Garcia^{*†}, Gary Johnson^{*¶}, Anna Baron^{*||}, Jie Yang^{**}, Theodore Puck^{*†.††}, and Paul Bunn, Jr.^{*†}

^{*}Lung Cancer Program, University of Colorado Cancer Center, the Departments of [†]Medicine, [§]Biochemistry, [¶]Pharmacology, and ^{||}Preventive Medicine and Biostatistics, University of Colorado Health Sciences Center, Denver, CO 80262; and ^{**}National Jewish Research Center, and ^{††}Eleanor Roosevelt Institute, Denver, CO 80206

Contributed by Theodore Puck, February 8, 2002

All small cell (SCLCs) and many non-small cell lung cancers (NSCLCs) have neuroendocrine features including production of neuropeptides and cell surface receptors creating autocrine and paracrine growth loops. Neuropeptides bind to a family of 7-transmembrane receptors and activate heterotrimeric G proteins consisting of $G_{\alpha q}$ and $G_{\alpha 12,13}$. Substance P derivatives (SPDs) induced apoptosis and inhibited growth of lung cancer cells by discoordinately inhibiting $G_{\alpha q}$ and stimulating $G_{\alpha 12,13}$. However, these SPDs had low potency and short half-lives. In this report we show that a bradykinin antagonist dimer, CU201, inhibited the growth of SCLC and NSCLC cell lines with or without multidrug-resistant proteins and was 10-fold more potent with a longer plasma half-life than SPDs. Bradykinin agonists in either monomeric or dimeric form and monomeric bradykinin antagonist have no effect on lung cancer cell growth. The dimeric linking moiety of the two molecules was created, requiring a sufficient number of carbon chains to provide critical spacing between the two antagonists. CU201 inhibited intracellular Ca^{2+} release in response to bradykinin, indicating blockage of the $G_{\alpha q}$ signal, and stimulated c-Jun kinases, indicating stimulation of the $G_{\alpha 12,13}$ pathway. CU201-induced apoptosis was preceded by unique changes in apparent nuclear DNA binding and by c-Jun kinase and caspase-3 activation. At the concentration at which CU201 inhibited the growth of the cancer cells, it had no effect on the growth of normal lung cells *in vitro*. CU201 and similar compounds offer hope of becoming a new form of targeted therapy for tumors with neuroendocrine properties.

Lung cancer is the leading cause of cancer death in men and women in the U.S. (1). Small cell lung cancer (SCLC) comprises 20% of lung cancer cases (2). Clinically, SCLCs are characterized by a propensity for early metastases and initial high response rates to chemotherapy and radiotherapy (2). Biologically, SCLCs are characterized by expression of neuroendocrine features including the production of neuropeptides coupled with expression of neuropeptide receptors, creating autocrine/paracrine growth loops (3–5). Many non-SCLCs (NSCLCs) and prostate, breast, and gastrointestinal cancers also express peptide receptors and respond to neuropeptide stimulation (6, 7). Autocrine growth stimulation by peptides led to the development of specific peptide inhibitors including monoclonal antibodies to growth factors or receptors and specific peptide antagonists (8–10). The low response rate to specific inhibitors was attributed to other peptides maintaining the autocrine loop when a single peptide was inhibited (8).

Each peptide binds to cell surface receptors of appropriate structure and activates a similar identical intracellular signaling pathway. This similarity created the possibility of developing compounds that would interfere with signals produced by multiple peptides. In SCLC, each 7-transmembrane-spanning peptide receptor is coupled to both $G_{\alpha q}$ and $G_{\alpha 12,13}$ heterotrimeric G proteins (8, 11–15). We and others showed that inhibition of the $G_{\alpha q}$ signal pathway (by transfection of GTPase-deficient $G_{\alpha q}$ genes or transfection of catalytically inactive phospholipase C- β genes) inhibited inositol triphosphate release, calcium flux, activation of protein

kinase C- α , calmodulin, and cell proliferation. Activation of $G_{\alpha 12,13}$ led to activation of c-Jun kinase and apoptosis (4, 12).

Some substance P derivatives (SPDs) were shown to inhibit growth of several SCLC cell lines *in vitro* and *in vivo* (11, 13, 15, 16). These SPDs initially were reported to be broad-spectrum antagonists, because they blocked the calcium response induced by multiple peptides of unrelated structures (5, 11, 15, 16). Subsequent studies showed that SPDs inhibited $G_{\alpha q}$ activation while simultaneously stimulating $G_{\alpha 12,13}$ signaling (11, 16, 17). These compounds were termed “biased agonists,” because they inhibited proliferative signals and stimulated apoptotic signals. However, SPDs required high concentrations to inhibit SCLC growth and did not inhibit the growth of NSCLCs. One of these SPDs, termed SPD-G, inhibited the growth of SCLC tumors in nude mice and has completed phase I testing with acceptable toxicity (18, 19). However, low potency and a short half-life hinder further clinical development. These limitations led to the search for alternative compounds.

The bradykinin (BK) receptor is expressed in most of the human lung cancer cell lines, and BK is one of the most potent neuropeptides that causes intracellular calcium flux in these SCLC and NSCLC cell lines (3). However, it shows only moderate mitogenic effects. We discovered that a dimeric BK antagonist (CP-127, bradycor) and related dimers produced modest growth inhibition of SCLC cell lines at high concentrations (8). Subsequently, we synthesized a series of novel, potent BK antagonist monomers and dimers and have now shown that one of the BK antagonist dimers, CU201, acts as a biased agonist, inhibits the growth of both SCLC and NSCLC cell lines by a unique mechanism, and has stability in serum. CU201 and related compounds may be useful in the treatment of lung cancers and other cancers with neuroendocrine features.

Methods and Materials

Cell Lines and Culture Conditions. The NSCLC line NCI-H157, the mesothelioma line H290, and the SCLC lines NCI-H345, -H69, -H209, -H740, -H1048, -H510, and -H82 were provided by J. Minna and A. Gazdar (University of Texas Southwestern Medical School, Dallas). The SCLC cell line SHP-77 was provided by A. Koros (University of Pittsburgh, Pittsburgh). The NSCLC line A549 and the normal lung fibroblast lines CCD-16LU and IMR90 were obtained from the American Type Culture Collection. Cell lines were maintained in RPMI medium 1640 (GIBCO/BRL Life Technologies, Grand Island, NY) supplemented with 10% FBS

Abbreviations: SCLC, small cell lung cancer; NSCLC, non-SCLC; SPD, substance P derivative; BK, bradykinin; MTT, modified tetrazolium test; GRP, gastrin-releasing peptide; JNK, c-Jun N-terminal kinase.

[†]To whom reprint requests should be addressed at: University of Colorado Cancer Center, Box B171, 4200 E, 9th Avenue, Denver, CO 80262. E-mail: Dan.Chan@UCHSC.edu.

The publication costs of this article were defrayed in part by page charge payment. This article must therefore be hereby marked “advertisement” in accordance with 18 U.S.C. §1734 solely to indicate this fact.

Structure of BK Antagonists

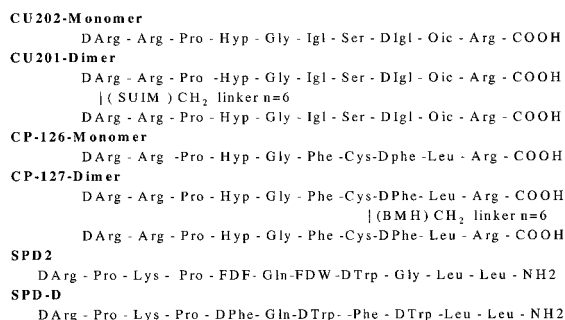


Fig. 1. Structures of CU202, CU201, SPD2, SPD-D, CP126, and CP127. Hyp, *trans*-4-hydroxyproline; Igl, α -(2-indanyl) glycine; Oic, octahydroindole-2-carboxylic acid; SUIM, suberimide linker; BMH, bismaleimido-hexane; FDF, 4-fluoro-D-phenylalanine; FDW, 5-fluoro-D-tryptophan.

(HyClone) or 10 nM hydrocortisone/5.0 μ g/ml insulin/10 μ g/ml transferrin/10 nM 17-estradiol/30 nM sodium selenite/100 units/ml penicillin/100 μ g/ml streptomycin (HITES medium, ref. 20). All cell lines were grown in 5% CO₂ incubators with 100% humidity.

Synthesis of BK Antagonist Peptides. Peptide antagonists were synthesized by the solid-phase method (21) using butyloxycarbonyl-amino acids and conventional side chain-blocking groups. Indanyl-glycine (D- α -(2-indanyl) glycine, L- α -(2-indanyl) glycine) was synthesized according to Gera and Stewart (22). Other unusual amino acids, D-1,2,3,4-tetrahydroisoquinoline-3-carboxylic acid and octahydroindole-2-carboxylic acid were purchased from Aldrich. Peptide amino acid analysis was characterized by thin layer chromatography and laser-desorption mass spectroscopy.

Synthesis of CU201 Dimers. Cross-linkers (dimethyl suberimide-2HCl, disuccinimidyl suberate, and bismaleimido-hexane) of varying carbon-chain lengths were purchased from Pierce. Homodimers were cross-linked from monomers in solution as described (23). The structures of the antagonists are shown in Fig. 1. Tohru Mochizuki and Noboru Yanaihara (University of Shizuoka, Shizuoka, Japan) provided SPD2 (Fig. 1). SPD-D (Fig. 1) was purchased from Bachem. A series of BK antagonist dimers with various cross-linkers was also obtained from Cortech (Denver, CO).

Calcium Flux Assays. Cells were loaded with the calcium indicator Indo-1/acetoxymethyl ester (Molecular Probes) according to methods described previously (4). Analysis was by flow cytometry using an EPICS 752 (Coulter) or the MoFlo (Fort Collins, CO) with UV excitation (80 mW at 350 nM) from a model INNOVA 90/5 argon ion laser (Coherent Radiation, Palo Alto, CA). Changes in intracellular calcium, [Ca²⁺]_i, levels were determined by quantifying changes in the ratio of 410-nM emission to 490-nM emission using 410 and 490 band-pass filters (Oriel, Stamford, CT; ref. 4).

c-Jun N-Terminal Kinase (JNK) Assays. Cells were lysed for 30 min at 4°C as described (24). Aliquots of cell extracts containing 200 μ g of protein were incubated for 2 h at 4°C with glutathione S-transferase-c-Jun (1-79) immobilized to glutathione-agarose. After the 2-h incubation, 20 μ M [γ -³²P]ATP (25,000 cpm/pmol) was added, and samples were incubated for 20 min at 30°C (26). The reactions were terminated, boiled, and submitted to 12% SDS/PAGE (13). The glutathione S-transferase-c-Jun (1-79) polypeptides were identified in Coomassie-stained gels, excised, and counted in a scintillation counter.

Cell Cycle Distribution and Apoptosis. Cell cycle distributions and percentage apoptosis was determined by flow cytometry. Cells

Table 1. Effects of CU201, CU202, and SPD2 on cell cycle distribution and apoptosis in SCLC and NSCLC cell lines after 24-h exposure

Cell line	Agent	%G ₁ /G ₀	%S	%G ₂ /M	%Apoptosis
SHP-77	Control	43	36	21	0.0
	CU201, 1.5 μ M	47	40	13	53.0
	CU202, 40 μ M	51	30	19	0.2
	SPD-D, 40 μ M	50	37	13	26.0
A549	Control	52	35	13	0.0
	CU201, 1.5 μ M	47	39	14	0.14
	CU202, 40 μ M	52	34	14	0.04
	SPD-D, 40 μ M	55	37	8	2.8

were stained with saponin/propidium iodide/RNase solution and analyzed by fluorescence-activated cell sorter using a Coulter EPICS and MODFIT LT software (Verity Software House, Topsham, MA; ref. 25).

Cytogenetic Analysis. To determine whether the two subpopulations detected by DNA content analysis represented distinct aneuploid clones, karyotypic analyses using G-banding and spectral karyotyping techniques were performed according to techniques described previously (26).

Activation of Caspase-3. After various treatments, cytosolic and mitochondrial fractions were isolated by differential centrifugation. ³⁵S-Labeled caspase-3, translated and purified as described (27), was incubated with cytosolic and mitochondrial fractions and dATP for 1 h at 37°C (27). At the end of the incubation period, the reaction was terminated, and the samples were submitted to 15% SDS/PAGE. The gel was transferred to a nitrocellulose filter and exposed to Kodak X-Omat AR film for 16 h at room temperature.

Detection of Apoptosis by Fluorescent Microscopy. After varying treatments, cells were stained with propidium iodide and bis-benzimide (Hoechst 33245) and examined for signs of apoptosis by fluorescent microscopy. More than 200 treated cells were scored (in duplicate) to establish the percentage of apoptotic cell death.

Modified Tetrazolium Test (MTT) Growth Assay. Cell growth was assessed by an MTT assay (28). The absorbency of each well was measured by using an automated plate reader (Molecular Devices). The data were analyzed by using a nonlinear mixed model with the SAS procedure PROC NL MIXED. This nonlinear mixed effect model distinguishes between variability between cell types and within the same cell type. The H_i (mean IC₅₀ for the *i*th cell type) then were compared with assessed differences between cell types.

Results

Effects of Peptides on DNA Content, Cell Cycle Distribution, and Apoptosis in SCLC and NSCLC Cell Lines (Table 1 and Fig. 2). When SHP-77 cells were exposed to varying concentrations of CU201 as low as 1.5 μ M, a new apparent “aneuploid” population of cells appeared by 8 h (Fig. 2A). This new population was consistent with a hyperdiploid G₁, S, and G₂/M. The fraction of cells in this apparent aneuploid population increased with increasing concentration and time through the first 24 h. By 24 h, this aneuploid population disappeared as a sub-G₁ population of apoptotic cells appeared, indicating the aneuploid cells were destined to become apoptotic (Fig. 2B).

To determine whether this new population of cells was truly aneuploid, G-banding and spectral karyotyping analysis were performed before and after CU201 exposure. Both specimens were near diploid, with chromosome numbers ranging from 44 to 50 and a modal chromosome number of 47. The 20% increase in DNA

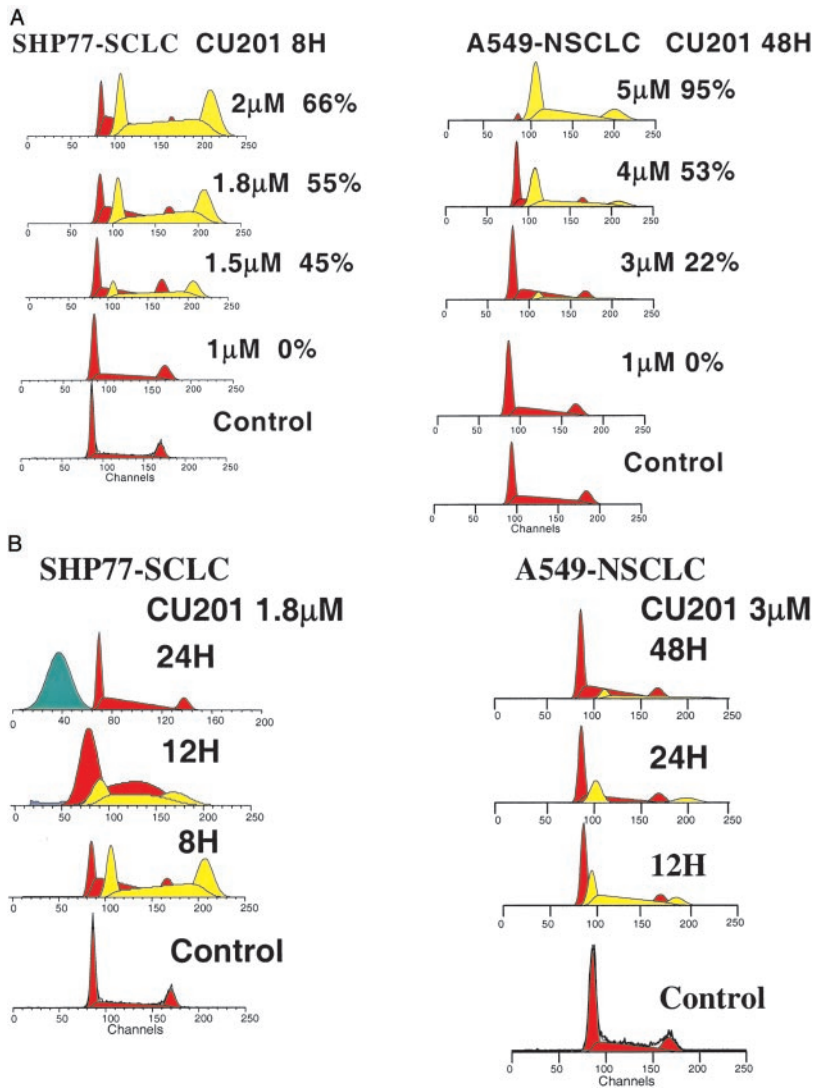


Fig. 2. (A) The effects of varying concentrations of CU201 on DNA content in SHP-77 SCLC after an 8-h exposure (*Left*) and in A549 NSCLC 48 h postexposure (*Right*). A new population appeared (lightly shaded area) and increased from 45 to 66%, with increasing concentration in the SHP-77 line, and from 22 to 95% in the A549 line. (B, *Left*) The aneuploid population that appeared at 8 h at 1.8 μM in the SHP-77 cells changed to a sub- G_1 apoptotic population between 12 and 24 h. (*Right*) The aneuploid population in A549 cells first appeared at 3.0 μM (12 h) and was maximal at 5.0 μM (24–48 h).

content of the aneuploid DNA peak in the treated population, if reflecting aneusomy, would increase the modal chromosome number from 47 to 56. We only observed a modal chromosome number of 47 and did not detect any changes in aneusomy. Extra copies of large chromosomes or gene amplification also would increase DNA content. However, multiple and complex chromosomal abnormalities observed in treated and untreated specimens were coincident, represented by derivative chromosomes. Therefore, we believe these peaks represent changes in DNA-propidium iodide binding induced by CU201 treatment that preceded further DNA changes associated with apoptosis.

CU201 produced similar changes in DNA content in three SCLC (SHP-77, H69, and H146) and two NSCLC (A549 and H157) cell lines tested. The NSCLC cell lines underwent similar changes at later time points and at slightly higher concentrations as shown for A549 cells in Fig. 2A and B. In contrast, neither SPD-D nor CU202 produced any changes in the population DNA content at concentrations up to 40 μM and up to 3 days of exposure. Table 1 shows the effects of CU201, CU202, and SPD-D on cell cycle distribution in SHP-77 SCLC and A549 NSCLC cells at 24 h. Other than the appearance and disappearance of this apparent aneuploid peak (high DNA index peak) in CU201-exposed cells, each of the agents produced few changes in cell cycle distribution. As shown in Table 1, small increases in the G_1 fraction were noted in SHP-77 cells exposed to CU202 and CU201 at 24 h, but this G_1 increase

disappeared by 48 h. Little change in cell cycle distribution was noted in A549 cells. An increase in apoptotic cells was noted early in cells exposed to CU201. The increase in apoptotic cells was dose- and time-dependent (Fig. 2.)

Effects of BK, SPD-D, CU202, and CU201 on Intracellular Calcium Flux in SCLC and NSCLC Cell Lines. BK produced a dose-dependent increase in $[\text{Ca}^{2+}]_i$ in both the SCLC (SHP-77, H69, and H146) and NSCLC (A549 and H157) cell lines, as shown for SHP-77 cells in Fig. 3A. BK (10 nM) alone was associated with a rapid rise in $[\text{Ca}^{2+}]_i$ in 84% of the cells (Fig. 3A). Each of the three antagonists alone, SPD-D, CU202, and CU201, produced no change in calcium flux. CU202 and CU201, at nM concentrations, completely abolished the BK-induced calcium flux. SPD-D did not inhibit the GRP-induced calcium flux completely even at 60 μM . As illustrated in Fig. 3A and B, CU201 at a concentration of 1 nM decreased the fraction of SHP-77 cells responding to BK from 84 to 68%. CU201 at 10 nM delayed the peak response to BK from 5 to 30 sec and further reduced the percentage of responding cells to 46%. CU201 at 100 nM completely abolished the response to BK. The IC_{50} (50% inhibition dose) for CU201 inhibition of BK-induced calcium flux was 10 nM (Fig. 3B). There were major differences in the potency of CU201, CU202, and SPD-D, as illustrated in Fig. 3. The concentration of CU202 required for complete BK inhibition was 1,000 nM, and the IC_{50}

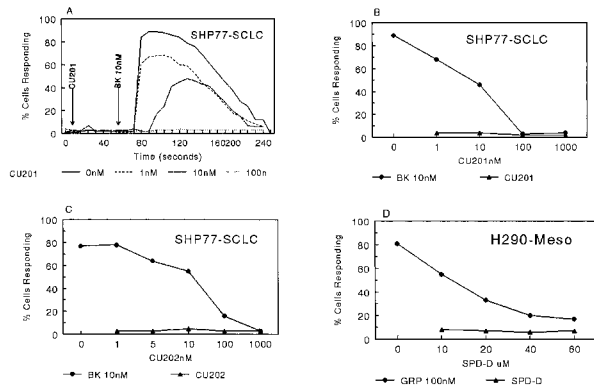


Fig. 3. Effects of SPD-D, CU202, and CU201 on BK-induced or gastrin-releasing peptide (GRP)-induced calcium flux. Meso, mesothelioma.

was 50 nM. On the contrary, SPD-D required a concentration of $>60 \mu\text{M}$ for complete GRP inhibition, and the IC_{50} was $12 \mu\text{M}$. The fraction of A549 NSCLC cells that respond to BK ($\approx 35\%$) was less than the fraction of responding SHP-77 cells. However, the two BK antagonists, CU202 and CU201, each completely inhibited the BK-induced response in A549 cells with similar IC_{50} values to those observed in SHP-77 cells (data not shown).

The peptide specificity of SPD-D, CU202, and CU201 was determined by their ability to inhibit the calcium flux induced by BK, GRP, and cholecystinin. The antagonists CU202 and CU201 specifically inhibited only the BK-induced calcium response in SHP-77 and A549 cells. Neither CU201 nor CU202 affected cholecystinin-induced calcium flux in NCI-H510 cells. GRP-induced calcium flux was almost completely inhibited by SPD-D, partly inhibited by CU201, and not inhibited by CU202 at all.

To determine serum and plasma stability, the antagonists were incubated in human serum or plasma for varying periods at 37°C and then evaluated for their ability to inhibit BK-induced calcium flux in SHP-77 cells. Both CP126 monomer and CP127 dimer (Bradycor) inhibited BK-induced calcium flux in SHP-77 cells, but the effect was diminished by a 4-h incubation in serum, and the effect had gone completely after a 24-h incubation. The SPD-D lost its inhibitory activity after <24 h of incubation in serum. In contrast, both CU202 and CU201 were extremely stable and could inhibit BK-induced calcium flux completely after incubation in human plasma or serum for >6 days.

Effects of BK, SPD2, SPD-D, CU202, and CU201 on JNK Activation. The effect of BK and GRP agonists and the four antagonists SPD2,

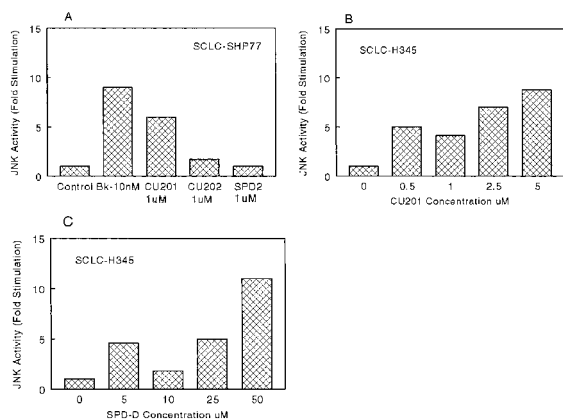


Fig. 4. Effects of SPD-D, CU202, and CU201 on JNK activity in SHP-77 and NCI-H345 SCLC cells.

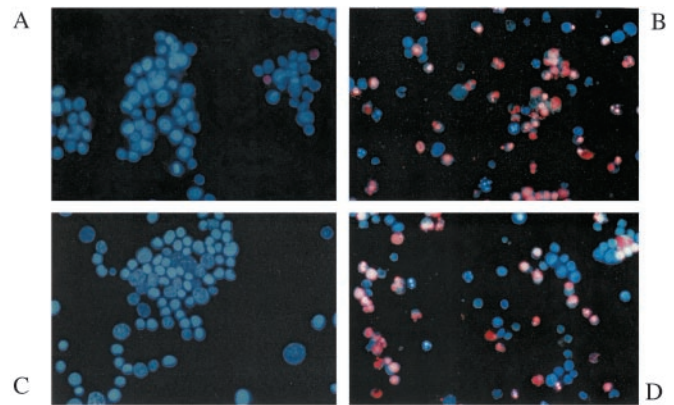


Fig. 5. Effects of CU201, CU202, and SPD2 on apoptosis in SHP-77 SCLC cells. (A) A fluorescence microscopic image of untreated SHP-77 cells. The lack of apoptosis induced by $40 \mu\text{M}$ CU202 is shown in C. The high level of apoptosis induced at 48 h by $3 \mu\text{M}$ CU201 is shown in B and by $40 \mu\text{M}$ SPD2 in D.

SPD-D, CU202, and CU201 on JNK activation were assessed in SHP-77 SCLC cells and H345 cells, respectively. In SHP-77 cells, BK and the BK antagonist CU201 ($1 \mu\text{M}$) produced 6–9-fold increases in JNK activation after 15 min of exposure (Fig. 4A). CU202 and SPD2 at $1 \mu\text{M}$ produced no effect on JNK activity in SHP-77 cells (Fig. 4A). The effect of CU201 and SPD-D on JNK activation in H345 cells is shown in Fig. 4B and C, respectively. Both CU201 and SPD-D increased JNK activation by 9–11-fold in H345 cells. However, CU201 was 10-fold more potent with an EC_{50} of $2 \mu\text{M}$ compared with an EC_{50} of $20 \mu\text{M}$ for SPD-D. Peak activation occurred at $5 \mu\text{M}$ for CU201 and $50 \mu\text{M}$ for SPD-D.

Effects of SPD2, CU201, and CU202 on Apoptosis and Caspase-3 Activation.

SPD2 and CU201 produced a dose- and time-dependent increase in apoptosis, whereas CU202 had no effect on apoptosis by fluorescence microscopy. Apoptosis induced by CU201 peaked at a concentration of $3 \mu\text{M}$ at 24–72 h (Fig. 5A). SPD2 produced a similar increase in apoptotic cells, but higher concentrations (20 – $40 \mu\text{M}$) were required, and apoptosis occurred at later time points (maximum of 48–72 h, Fig. 5B). To study the mechanism of apoptosis further, we assessed the activation of caspase-3 from cytosolic and mitochondrial fractions of SHP-77 cells exposed to SPD2, CU202, and CU201 for 24 h. Both SPD2 and CU201 produced activation of caspase-3, whereas CU202 failed to activate caspase-3 (Fig. 6).

Effects of SPD2, SPD-D, CU201, and CU202 on Cell Growth of SCLC and NSCLC Cells in MTT Assays (Fig. 7). Growth inhibition of SCLC and NSCLC lines by SPD2, SPD-D, CU201, and CU202 was evaluated by using MTT assays. CU201 inhibited the growth of both SHP-77

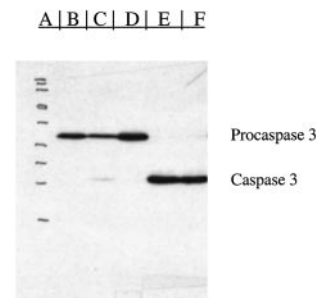


Fig. 6. The induction of caspase-3 by $3 \mu\text{M}$ CU201 (lane E) and by $40 \mu\text{M}$ SPD2 (lane F) in SHP-77 is shown. Lane A shows molecular weight markers, and lanes B–D are controls.

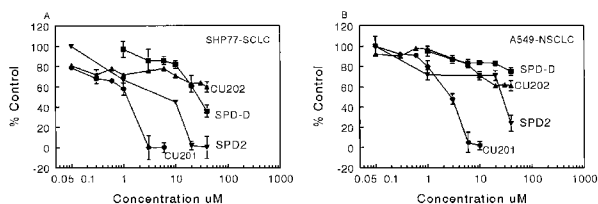


Fig. 7. Effects of CU201, CU202, SPD2, and SPD-D on growth inhibition of SHP-77 and A549 cell lines by MTT assay.

($IC_{50} = 1 \mu M$) and A549 ($IC_{50} = 3 \mu M$; Fig. 7). SPD2 and SPD-D also inhibited the growth of SHP-77 SCLC cells but were less potent. The IC_{50} for growth inhibition of the SHP-77 SCLC was $8 \mu M$ for SPD2 and $12 \mu M$ for SPD-D. SPD2 and SPD-D affected the growth of A549 NSCLC cells only at concentrations $>20 \mu M$; the IC_{50} for SPD2 was $30 \mu M$, and the IC_{50} for SPD-D was $>40 \mu M$ (Fig. 7). CU202 had modest growth-inhibitory effects on the growth of SHP-77 or A549 cell lines and only at $40 \mu M$ (Fig. 7). The CU201 IC_{50} for growth inhibition was similar to its EC_{50} for JNK activation in SHP-77 cells and much lower than the IC_{50} and EC_{50} of the SPDs for these parameters. CU201 effects on the growth of various cell lines are summarized in Table 2. Two normal human lung fibroblast cell lines, IMR90 and CCD-16Lu, were treated with CU201, and the IC_{50} was found to be 7 and $5.3 \mu M$, respectively. Nine SCLC cell lines were tested; two of these expressed multidrug-resistant protein, lung-resistant protein, or multidrug-resistant protein-1. Complete growth inhibition was achieved in all nine lines. The average IC_{50} was $2.1 \pm 0.41 \mu M$ for all cell lines including $2.3 \pm 0.46 \mu M$ for the seven lines without multidrug-resistant protein, lung-resistant protein, or multidrug-resistant protein-1 overexpression and $1.3 \pm 0.3 \mu M$ for the two cell lines overexpressing drug-resistance proteins. There were no statistical differences between cell lines with and without drug-resistant protein expression. CU201 also produced complete growth inhibition in all five NSCLC cell lines with an average IC_{50} of $4.1 \pm 0.58 \mu M$. The IC_{50} for the five NSCLC cell lines was significantly higher than the nine SCLC cell lines ($P = 0.0081$). The IC_{50} was $3.7 \pm 0.3 \mu M$ in three NSCLC cell lines without drug-resistance proteins and $4.8 \pm 0.5 \mu M$ in the two NSCLC cell lines expressing one or more of these proteins. CU201 also inhibited the growth of five prostate cancer cell lines ($IC_{50} = 3.0 \pm 0.58 \mu M$) and

Table 2. CU201 growth inhibition of cell lines of different histology

Cell type	n	Average IC_{50} , μM	Range, μM
Normal lung cell lines*	2	6.2	5.3–7.0
SCLC†	9	2.1	1.0–3.5
SHP-77‡		1.0	
H69‡		1.0	
H69VPR2‡		1.5	
NSCLC§	5	4.1	1.0–5.0
SW1573		5.0	
SW2R120¶		4.5	
SW2R160¶		5.0	
Prostate carcinomas	5	3.0	3.3–5.3
Breast** carcinomas	5	2.6	1.3–3.9

*Normal lung fibroblast cell lines: IMR90 and CCD-16Lu.

†SCLC: H69, H69VPR2, H209, H345, H740, H82, SHP-77, DMS114, and H1048.

‡SCLC: SHP-77 overexpresses multidrug-resistant protein (not drug selected *in vitro*; ref. 29); H69-parental, H69VPR2 overexpresses multidrug-resistant protein (drug selected *in vitro*; ref. 30).

§NSCLC: A549, H157, SW1573, SW2R120, and SW2R160.

¶NSCLC: SW1573-parental, SW2R120, and SW2R160 overexpress lung-resistant protein (drug selected *in vitro*; ref. 31).

||Prostate carcinomas: LNCaP, DU145, TSU, PC3, and PPC1.

**Breast carcinomas: ZR75, T47DV, MDAMB231, MCF7, and SKBR3.

Table 3. Effect of linker length of BK dimers on growth inhibition of SHP-77 SCLC cells

Linker length	Growth inhibition, $40 \mu M$	IC_{50} , μM
2	0%	NA
4	0%	NA
6*	0%	NA
8	60%	30
9	100%	10
10	100%	5
12	100%	10

NA, not applicable.

*CP127.

five breast cancer cell lines ($IC_{50} = 2.6 \pm 0.88 \mu M$). The differences in IC_{50} values between SCLC and breast ($P = 0.34$) and SCLC and prostate ($P = 0.19$) cancer cell lines were not significant. The differences in IC_{50} values between NSCLC and breast ($P = 0.074$) and prostate ($P = 0.19$) cancer cell lines also was not significant.

Effect of Linker Length on Growth Inhibition by BK Antagonist Dimers.

Because antagonist dimers inhibited lung cancer growth and monomers did not, we studied the effect of linker length effect on growth by varying the number of carbon units used in producing a homodimer. Monomeric Cys-containing antagonist CP126 (Fig. 1) was cross-linked via bis-maleimides and the number of carbon (CH_2) groups joining the maleimides varied from 2 to 12. Dimers having carbon chain lengths of 2, 3, 4, or 6 units produced little or no growth inhibition (Table 3). CP127 has a linker length of six methylene groups (Fig. 1). Significant growth inhibition was observed first with a linker length of eight methylene groups, which produced 60% growth inhibition at $40 \mu M$. Maximal growth (100%) inhibition occurred with dimers of nine methylene groups with an IC_{50} of $10 \mu M$. Compounds with 10–12 methylene groups also produced 100% growth inhibition but without further improvement in potency (IC_{50} values of 5–10 μM), suggesting growth inhibition saturated when the linker reached the nine methylene groups. For BK antagonist CU201 that is linked at the N terminus rather than at the Cys-8 (Fig. 1), a shorter linker length ($n = 6$) was sufficient to provide maximal growth inhibition. Another BK antagonist dimer linked at the N-terminal in the same manner as CU201 with a longer linker ($n = 10$) gave 100% growth inhibition without further improvement in potency compared with CU201 (data not shown). Interestingly, dimers cross-linked at the N terminus using the same cross-linker but consisting of two dummy molecules (peptides with scrambled sequences), one active BK antagonist and one dummy molecule, or two active BK agonists (CU202) did not produce growth inhibition.

Discussion

Neuropeptides play a prominent role in the autocrine growth of SCLC and a variety of other carcinomas. In this paper we show that a novel BK antagonist dimer, CU201, inhibited the growth of lung cancer cell lines of all histologies irrespective of the expression of drug-resistance proteins. CU201 inhibited the calcium flux induced by BK and other peptides, activated JNK and caspase-3, and induced a unique form of apoptosis. CU201-induced apoptosis included early changes in DNA binding, activation of JNK, and subsequent activation of caspase-3. Interestingly, the monomeric antagonist, CU202, inhibited BK-induced calcium flux but failed to activate JNK pathways. It did not affect DNA binding or activate caspase-3 and apoptosis, and it did not inhibit growth. CU201 was stable in serum for more than 96 h. These findings indicate that CU201 is unique and should be developed as a possible targeted therapy for lung cancer and other cancers with a neuroendocrine phenotype.

The CU201-induced growth inhibition depended on the optimal separation of the molecules and a requirement for two active antagonistic molecules. Dimers consisting of two active BK agonists, two inactive dummy molecules, or one active BK antagonist and one inactive molecule did not inhibit cancer cell growth. The requirement of optimal physical separation of two active BK antagonistic molecules to achieve growth inhibition may imply the involvement of physically spaced receptors or dimerization of two BK receptors, although we do not have direct evidence supporting receptor dimerization. Homo- and heterodimerization of the 7-transmembrane G protein-coupled receptors have been reported recently for a γ -aminobutyric acid receptor (32), β -adrenergic receptor (33), and muscarinic receptor (34). The requirement of an optimal physical separation of two functional antagonists indirectly suggests that the G protein-coupled BK receptors may be dimerized in the presence of CU201. Estimation shows that the cross-linker used in the CU201 is just long enough to cross over two transmembrane helices, assuming that two BK receptors are aligned side by side in close proximity. The requirement of two linked active antagonists suggests that if the BK receptors become dimerized because of the binding of CU201, the primary antagonistic structures also play an important role in triggering the apoptotic signals. The constraint created by the critical cross-linker may force the antagonist molecules to interact within the BK receptors in a very specific manner that eventually leads to the apoptotic pathway. This interaction, however, is not shared with the dimeric agonists probably because of the subtle differences in their primary structures. It should be pointed out also that the dimeric compounds would have increased free energy of binding as compared with the monomers.

In this paper, we show that CU201 activated the JNK pathway, and caspase-3 stimulated apoptosis, inhibited the phospholipase C- β pathway, and inhibited the growth of different lung cancer cell lines. Moreover, CU201 was more potent than SPDs in each of these actions. The IC_{50} was 10-fold lower for CU201 than for the SPDs, and the serum half-life of CU201 was considerably longer. These studies suggest that CU201, similar to the SPDs, acts as a biased agonist on peptide receptor-G protein interactions in lung cancer cell lines.

CU201 consistently induced apoptosis in both SCLC and NSCLC cell lines. Activation of JNK, alterations in DNA structure, and activation of caspase-3 preceded apoptosis. The CU201-induced EC_{50} for activation of JNK and caspase-3 and the IC_{50} for growth inhibition were similar, whereas the IC_{50} for inhibition of peptide-induced calcium flux was much lower. The same was true for SPD2, although it was less potent for each activity. Thus, it is highly likely that induction of apoptosis played a major role in growth inhibition. The importance of changes in JNK activation, caspase-3 activation, and apoptosis on growth inhibition is supported also by the fact that the monomer CU202 inhibited BK-induced calcium flux but failed to affect JNK, DNA content, caspase-3, apoptosis, or growth. The alterations in DNA structure resulting in increased propidium iodide binding properties that preceded the apoptosis are unique and not described for other apoptosis-inducing agents.

Earlier studies showed that the 2A11 anti-GRP antibody inhibited SCLC growth *in vitro* and *in vivo* and produced an objective response in a patient with SCLC (7, 8). However, response rates were low in both preclinical models and the one clinical trial (6, 8). The SPDs were developed clinically, because they blocked the activity of several neuropeptides and inhibited the growth of a variety of SCLC cell lines. SPDs have completed phase I testing in humans. The problems facing the clinical development of the SPDs are a requirement for high concentrations to inhibit the growth of SCLC cells, their lack of inhibition of NSCLC cell lines and their short half-life in human serum. CU201 inhibited the growth of both SCLC and NSCLC cell lines and had a 10-fold greater potency and longer serum stability.

Our studies suggest that CU201 should be studied further as a targeted therapy for lung cancer. Additional preclinical studies are being conducted in collaboration with the National Cancer Institute through their Rapid Advancement of Investigational Drugs program. CU201 is a large peptide with chemically linked dimers. Large-scale production is expensive because of the cost of the artificial amino acids and the inefficiency of the linker chemistry. The development of peptidomimetics with a similar mechanism of action to reduce size and cost is being studied.

This work was supported in part by National Cancer Institute Grants CA 46934, CA 58187, and CA78154-01.

- Greenlee, R. T., Hill-Harmon, M. B., Murray, T. & Thun, M. (2001) *CA Cancer J. Clin.* **51**, 15–36.
- Cook, R. M., Miller, Y. E. & Bunn, P. A. (1993) *Curr. Probl. Cancer* **17**, 71–141.
- Bunn, P. A., Jr., Chan, D. C., Dienhart, D. G., Tolly, R., Togawa, M. & Jewett, P. B. (1991) *Cancer Res.* **52**, 24–31.
- Bunn, P. A., Jr., Dienhart, D. G., Chan, D. C., Puck, T. T., Togawa, M., Jewett, P. B. & Braunschweiger, E. (1990) *Proc. Natl. Acad. Sci. USA* **87**, 2162–2166.
- Sethi, T. & Rozengurt, E. (1991) *Cancer Res.* **51**, 3621–3623.
- Moody, T. W., Zia, F., Venugopal, R., Fagarasan, M., Oie, H. & Hu, V. (1996) *J. Cell Biochem.* **24**, 247–256.
- Siegfried, J. M., Krishnamachary, N., Gaither-Davis, A., Gubish, C., Hunt, J. D. & Shriver, S. P. (1999) *Pulm. Pharmacol. Ther.* **12**, 291–302.
- Chan, D. C., Geraci, M. & Bunn, P. A., Jr. (1998) *Drug Resist. Updat.* **1**, 377–388.
- Cuttitta, F., Carney, D. N., Mulshine, J., Moody, T. W., Fedorko, J., Fischler, A. & Minna, J. D. (1985) *Nature (London)* **316**, 823–826.
- Kelley, M. J., Linnoila, R. I., Avis, I. L., Georgiadis, M. S., Cuttitta, F., Mulshine, J. L. & Johnson, B. E. (1997) *Chest* **112**, 256–261.
- Jarpe, M. B., Knall, C., Mitchell, F. M., Buhl, A. M., Duzic, E. & Johnson, G. L. (1998) *J. Biol. Chem.* **273**, 3097–3104.
- Heasley, L. E., Zamarripa, J., Storey, B., Helfrich, B., Mitchell, F. M., Bunn, P. A., Jr. & Johnson, G. L. (1996) *J. Biol. Chem.* **271**, 349–354.
- Mitchell, F. M., Heasley, L. E., Qian, N.-X., Zamparripa, J. & Johnson, G. L. (1995) *J. Biol. Chem.* **270**, 1–6.
- Beckman, A., Helfrich, B., Bunn, P. A., Heasley, L. E. (1998) *Cancer Res.* **58**, 910–913.
- MacKinnon, A. C., Waters, C., Jodrell, D., Haslett, C. & Sethi, T. (2001) *J. Biol. Chem.* **276**, 28083–28091.
- Reeve, J. G. & Bleehan, N. M. (1994) *Biochem. Biophys. Res. Commun.* **199**, 1313–1319.
- MacKinnon, A. C., Armstrong, R. A., Waters, C. M., Cummings, J., Smyth, J. F., Haslett, C. & Sethi, T. (1999) *Br. J. Cancer* **80**, 1026–1034.
- Seckl, M. J., Higgins, T., Widmer, F. & Rozengurt, E. (1997) *Cancer Res.* **57**, 51–54.
- Jones, D. A., Cummings, J., Langdon, S. P., Maclellan, A. J., Higgins, T., Rozengurt, E. & Smyth, J. F. (1996) *Br. J. Cancer* **73**, 715–720.
- Carney, D. N., Bunn, P. A., Jr., Gazdar, A. F., Pagan, J. A. & Minna, J. D. (1981) *Proc. Natl. Acad. Sci. USA* **78**, 3185–3189.
- Stewart, J. M. & Young, J. D. (1984) in *Solid Phase Peptide Synthesis* (Pierce, Rockford, IL), 2nd Ed.
- Gera, L. & Stewart, J. M. (1996) *Immunopharmacology* **33**, 174–177.
- Gera, L., Stewart, J. M., Whalley, E., Burkard, M. & Zuzack, J. S. (1996) *Immunopharmacology* **33**, 178–182.
- Hibi, M., Lin, A., Smeal, T., Minden, A. & Karin, M. (1993) *Genes Dev.* **7**, 2135–2148.
- Yamamura, Y., Rodriguez, N., Schwartz, A., Eylar, E., Bagwell, B. & Yano, N. (1995) *Cell Mol. Biol.* **41**, S121–S132.
- Van Bokhoven, A., Varella-Garcia, M., Korch, C. & Miller, G. J. (2001) *Cancer Res.* **67**, 6340–6344.
- Liu, X., Kim, C. N., Yang, J., Jemerson, R. & Wang, X. (1996) *Cell* **86**, 147–157.
- Carmichael, J., Mitchell, J. B., DeGraff, W. G., Gamson, J., Gazdar, A. F., Johnson, B. E., Glatstein, E. & Minna, J. D. (1988) *Br. J. Cancer* **57**, 540–547.
- Soriano, A. F., Helfrich, B., Chan, D. C., Heasley, L. E., Bunn, P. A. & Chou, T. C. (1999) *Cancer Res.* **59**, 6180–6184.
- Glisson, B. S. & Alpeter, M. D. (1992) *Anticancer Drugs* **4**, 359–366.
- Kuiper, C. M., Broxterman, H. J., Baas, F., Schuurhuis, G. J., Haisma, H. J., Scheffer, G. L., Lankelma, J. & Pinedo, H. M. (1990) *J. Cell. Pharmacol.* **1**, 35–41.
- Kuner, R., Kohr, G., Grunewald, S., Eisenhardt, G., Bach, A. & Kornau, H. C. (1999) *Science* **283**, 74–77.
- Hebert, T. E., Moffett, S., Morello, J. P., Loisel, T. P., Bichet, D. G., Barret, C. & Bouvier, M. (1996) *J. Biol. Chem.* **271**, 16384–16392.
- Maggio, R., Barbier, P., Fornai, R., Corsini, G. U. (1996) *J. Biol. Chem.* **271**, 31055–31060.